

Superconductivity and antiferromagnetic ordering in the high-field paramagnetic oxypnictide $\text{NdFeAsO}_{0.94}\text{F}_{0.06}$

Chiara Tarantini,¹ Alex Gurevich,¹ David C. Larbalestier,¹ Zhi-An Ren,² Xiao-Li Dong,² Wei Lu,² and Zhong-Xian Zhao²¹National High Magnetic Field Laboratory, Florida State University, Tallahassee, Florida 32310, USA²National Laboratory for Superconductivity, Institute of Physics and Beijing National Laboratory for Condensed Matter Physics, Chinese Academy of Sciences, P.O. Box 603, Beijing 100190, People's Republic of China

(Received 1 October 2008; published 3 November 2008)

We present measurements of the temperature and field dependencies of the magnetization $M(T, H)$ of $\text{NdFeAsO}_{0.94}\text{F}_{0.06}$ at fields up to 33 T to probe the coexistence of superconductivity with global antiferromagnetic ordering. Although $M(T, H)$ at $48 < T < 140$ K exhibits a clear Curie-Weiss temperature dependence corresponding to the Neel temperature $T_N \approx 11\text{--}12$ K, the behavior of $M(T, H)$ below T_c is only consistent with either paramagnetism of weakly interacting magnetic moments or perhaps a spin-glass state. We show that the anomalous magnetic behavior of the high-field paramagnetic superconductor $\text{NdFeAs}(\text{O}_{1-x}\text{F}_x)$ is mostly determined by the magnetic Nd^{3+} ions, which rules out intrinsic long-range antiferromagnetism on the FeAs plane in the superconducting state.

DOI: [10.1103/PhysRevB.78.184501](https://doi.org/10.1103/PhysRevB.78.184501)

PACS number(s): 74.25.Ha, 74.70.Dd, 75.50.Ee

I. INTRODUCTION

The recently discovered superconducting oxypnictides¹ exhibit a coexistence of high critical temperatures $T_c \approx 26\text{--}57$ K with strong antiferromagnetic (AF) correlations and extremely high upper critical fields.² Neutron,^{3,4} μSR ,^{5,6} and NMR (Refs. 7 and 8) studies of undoped parent compounds have revealed a spin-density wave instability on FeAs planes at $T_N \approx 140\text{--}150$ K accompanied by a drop in the normal-state resistivity $\rho(T)$, and orthorhombic distortions of the tetragonal lattice.⁹ Doping with F or O reduces T_N and seemingly eliminates manifestations of these transitions in $\rho(T)$ of optimally doped oxypnictides.^{10,11} Yet an unresolved question remains if magnetic correlations can provide a global AF order at lower temperatures in the superconducting state, which would be important for distinguishing between different pairing mechanisms.^{12–16} However, detecting any putative AF state below T_c by standard measurements of low-field magnetization $M(T, H)$ is very difficult because the AF response would be screened by the superconducting vortex state. This problem can be resolved by applying high magnetic fields which both weaken the superconducting response and enhance the paramagnetic magnetization. Moreover, high fields can destroy antiferromagnetism, resulting in distinctive cusps in the susceptibility $\chi(H, T)$ and jump wise spin-flip transitions. Such behavior of $\chi(H, T)$ would reveal any global AF state with the Neel temperature $T_N \lesssim \mu_B H / k_B$, where μ_B is the Bohr magneton. In this paper we search for manifestations of the field-induced breakdown of a global AF state in $\text{NdFeAs}(\text{O}_{0.94}\text{F}_{0.06})$, reporting measurements of $M(T, H)$ at high fields up to 33 T, which can destroy AF states with $T_N \lesssim 22$ K.

Our measurements of $M(T, H)$ in a wide range of fields $0 < H < 33$ T and temperatures $4.2 < T < 140$ K have shown a strong paramagnetic contribution to $M(T, H)$ both at $T > T_c$ and $T < T_c$. In the normal state $M(T)$ exhibits Curie-Weiss behavior with an apparent Neel temperature $T_N \approx 11\text{--}12$ K, which might suggest the coexistence of superconductivity and antiferromagnetism. However, $M(T, H)$ at

$T < T_c$ turns out to be inconsistent with long-range AF order, indicating that superconductivity effectively cuts off the AF correlations evident at $T > T_c$. In that respect $\text{NdFeAs}(\text{O}_{1-x}\text{F}_x)$ may be regarded as a paramagnetic superconductor similar to $\text{Nd}_{1.85}\text{Ce}_{0.15}\text{CuO}_4$ (Ref. 17) with a magnetic behavior different not only from most conventional superconductors but also from $\text{LaFeAs}(\text{O}_{1-x}\text{F}_x)$ oxypnictide. This difference may result from the large magnetic moment $\mu = 3.62\mu_B$ of a free Nd^{3+} ion, as compared to $\mu = 0$ for La^{3+} and $\mu = 1.5\mu_B$ for Sm^{3+} .¹⁸ We show that $M(T, H)$ of $\text{NdFeAs}(\text{O}, \text{F})$ is mostly dominated by the Curie-Weiss paramagnetism of Nd^{3+} with no apparent signs of AF ordering of either Nd^{3+} or Fe^{2+} down to 4.2 K.

II. SAMPLES

The $\text{NdFeAs}(\text{O}_{0.94}\text{F}_{0.06})$ polycrystalline samples were made as described previously.¹⁹ The sample with approximate dimensions of $1.4 \times 1 \times 0.5$ mm³, volume $V \approx 0.7$ mm³, and weight ≈ 4.5 mg had $\rho(T_c) \approx 0.53$ m Ω cm, $T_c \approx 49$ K, and about 90% of the theoretical density, 7.21 g/cm³. The susceptibility $\chi(T, H)$ and magnetic moment $M(T, H)V$ were measured by a superconducting quantum interference device (SQUID) magnetometer, vibrating sample magnetometers (VSMs) in a 14 T superconducting magnet, and a resistive 33 T dc magnet at the National High Magnetic Field Laboratory. Shown in Figs. 1 and 2 are the zero-field cooled (ZFC) and field cooled (FC) $M(T)$ curves, which change radically upon increasing field. For $H = 10$ mT, $M(T)$ exhibits a standard superconducting behavior with diamagnetic onset close to T_c . However, increasing field to only 0.5 T shrinks the irreversible diamagnetic loop while significantly increasing the paramagnetic component of $M(H)$. Further increase in H to 1.5 T practically eliminates the difference between the ZFC and FC curves, resulting in a strong paramagnetic behavior shown in more detail in Fig. 2.

III. PARAMAGNETIC RESPONSE

To gain an insight into the nature of the paramagnetic signal not masked by superconductivity, the magnetic mo-

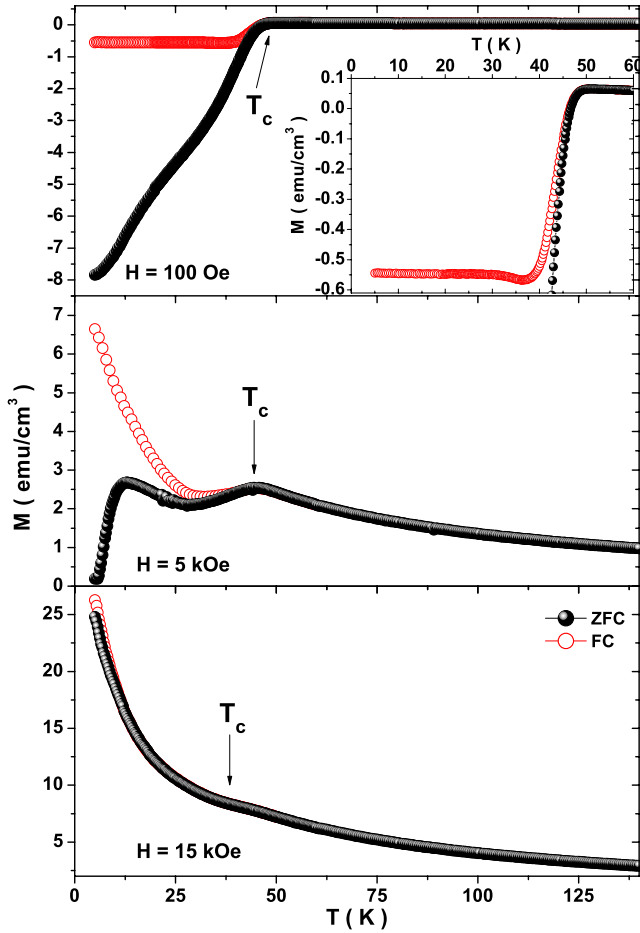


FIG. 1. (Color online) ZFC (black full dots) and FC [red (dark gray) open dots] $M(T)$ at 0.1, 5, and 15 kOe. The inset shows FC $M(T)$ at 0.1 kOe.

ment $M(T, H)$ was measured from 55 to 140 K. The results presented in Fig. 3 show the classic AF Curie-Weiss behavior, $M^{-1} \propto T + T_m$ with $T_m \approx 11-12$ K being practically independent of H at $0 < B < 5$ T. Such temperature dependence of $M(T, H)$ suggests AF ordering at $T_N \approx T_m$, below the su-

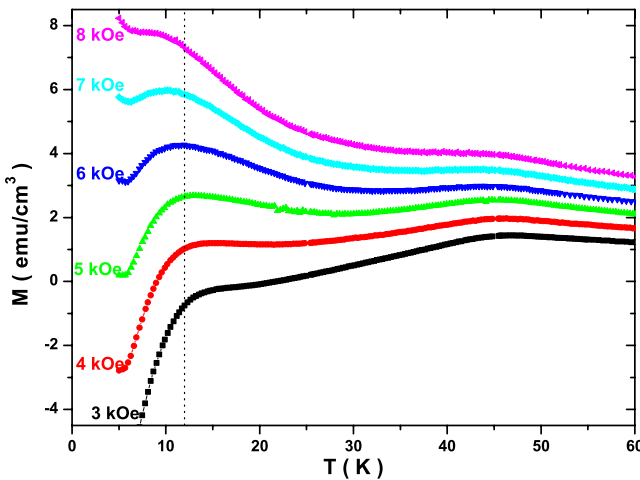


FIG. 2. (Color online) ZFC magnetization at different fields. The dash line shows T_m extracted from the data in Fig. 3.

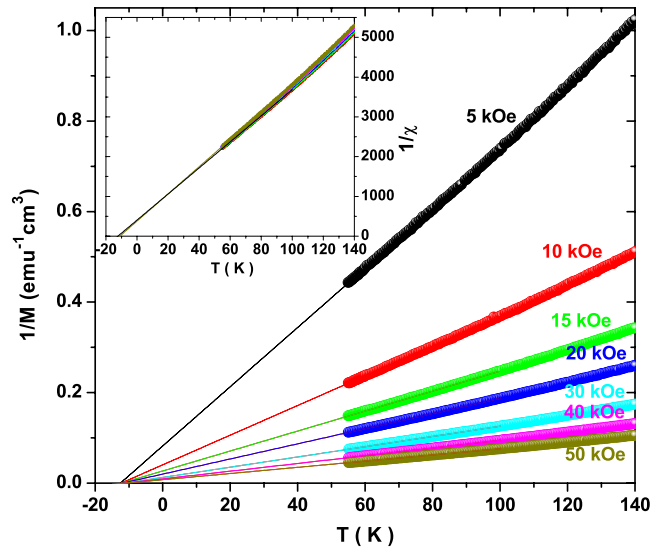


FIG. 3. (Color online) The AF Curie-Weiss linear temperature dependence of $M^{-1}(T, H) \propto T + T_m$ measured by SQUID. The linear extrapolations define $T_m \approx 11-12$ K. The inset shows the collapse of the inverse susceptibilities $\chi^{-1}(T, H) = H/M$ for different fields $0 < H < 5$ T onto a single straight line.

perconducting transition, and a coexistence of superconductivity and antiferromagnetism. To see if this is indeed the case, we measured $M(T, H)$ below T_c at high magnetic fields so as to suppress the magnetization due to pinned vortices and to probe $M(T, H)$ in the superconducting state at fields sufficient to destroy this putative AF state.

Shown in Fig. 4(a) is the $M(H)$ loop at 4.2 K. One can clearly see a superconducting hysteresis loop on top of a strongly paramagnetic, field-dependent background. Taking the mean value of the two branches of $M(B)$ as the paramagnetic magnetization $M_p = (M_\uparrow + M_\downarrow)/2$ added to the small reversible magnetization of the vortex lattice, we define the magnetization $\Delta M = M_\uparrow - M_\downarrow$ due to the critical state of pinned vortices. Using the Bean model,²⁰ we estimate the global critical current density $J_c(4.2 \text{ K}) \sim 10 \text{ kA/cm}^2$ at self field, taking the sample dimensions as length scales of magnetization current loops. Shown in Fig. 4(b) is $M(H, T)$ measured at higher fields up to 33 T and different temperatures. Here $M(4.2 \text{ K}, H)$ saturates above 15 T while $M(T, H)$ for higher temperatures increases very slowly as H increases. The width of the superconducting loop decreases as T and H increase, consistent with the usual behavior of $J_c(H, T)$.

To understand the observed $M_p(T, H)$ and the AF breakdown by magnetic field, we used the mean-field theory in which two magnetic sublattices with magnetizations M_1 and M_2 are controlled by the self-consistent fields $H_1 = H + aM_1 - bM_2$ and $H_2 = H + aM_2 - bM_1$, where the Weiss constants a and b quantify the exchange interaction with these sublattices.¹⁸ The self-consistency equations, $2M_i = M_0 B_J(\mu H_i/T)$, $i=1,2$, determine the net magnetization, $M(T, H) = M_1 + M_2$, and the AF order parameter $L(T, H) = M_1 - M_2$, where $M_0 = n\mu$, μ is an elementary magnetic moment, n is their density, $B_J(z) = [(2J+1)/2J] \coth[(2J+1)z/2J] - (1/2J) \coth(z/2J)$ is the Brillouin function, and J is the magnetic quantum number. For $T \gg T_N$, this model gives

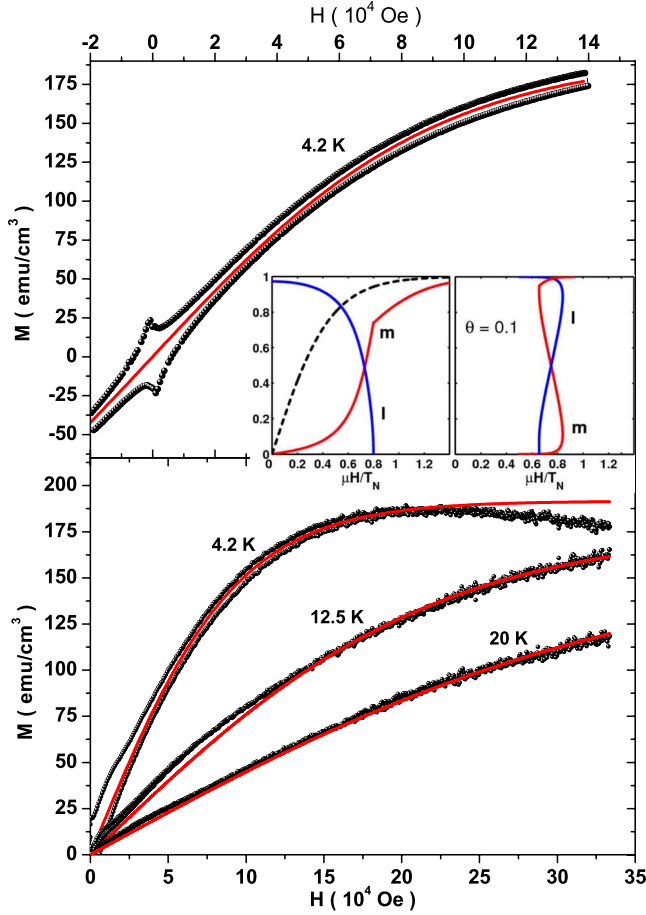


FIG. 4. (Color online) (a) Low-field $M(H)$ loop measured by VSM at 4.2 K and H perpendicular to the broader sample face. The red (dark gray) line shows $M=M_0 \tanh(\mu B/T)$ with $B=H+4\pi M$, $M_0=\mu n$ for $\mu=0.69\mu_B$, $M_0V=0.135$ emu, and $n=3 \times 10^{22}$ cm $^{-3}$. The inset shows $m(H)$ and $l(H)$ calculated from Eqs. (2)–(6) for $\gamma=0.5$, and $m=\tanh(h)$ (dashed line). Here the left panel shows the second-order transition for $\theta=5/11$, and the right panel shows the first-order metamagnetic transition for $\theta=0.1$. (b) High-field $M(H)$ loops at different T . The red (dark gray) lines show $M=M_0 \tanh(\mu B/T)$ with $\mu=0.67\mu_B$, $M_0V=0.133$ emu, and $n=3.1 \times 10^{22}$ cm $^{-3}$ (4.2 K); $\mu=0.85\mu_B$, $M_0V=0.123$ emu, and $n=2.25 \times 10^{22}$ cm $^{-3}$ (12.5 K); $\mu=0.85\mu_B$, $M_0V=0.112$ emu, and $n=2.05 \times 10^{22}$ cm $^{-3}$ (20 K).

$$\frac{\chi(T_*)}{\chi(T, H)} = \frac{T + T_m(H)}{T_* + T_m(H)}. \quad (1)$$

Here $T_m=(b-a)M_0(J+1)/6J$, $T_*=2T_m$, $T_m(B)=[1-c_f(\mu H/T)^2]T_m$, $c_f=(2J^2+2J+1)/10J^2$, and $\chi(T_*)=9JT_m/(J+1)\mu M_0$, $T_m=\gamma T_N$ where $\gamma=(b-a)/(b+a) < 1$. Equation (1) describes the data in Fig. 3 well, allowing us to estimate the density n of magnetic moments μ , which can provide the observed χ . Taking $\chi_0=n\mu^2/3T_m=1/395$ from the inset of Fig. 3, $T_m=12$ K, and $\mu=3.62\mu_B$ for Nd $^{3+}$,¹⁸ we obtain $n=3T_m\chi_0/\mu^2 \approx 1.5 \times 10^{22}$ cm $^{-3}$, close to the density of Nd atoms. Since the strong paramagnetism above T_c is only consistent with an atomic density of magnetic moments $\mu \approx 3\mu_B-4\mu_B$, it appears that Fe $^{2+}$ with much smaller $\mu \approx 0.25\mu_B-0.35\mu_B$ (Refs. 3 and 4) may only add a few per-

cent to $\chi \propto \mu^2$. However, the situation is more complicated because the large moments of free Nd $^{3+}$ ions do not survive in the crystal field of surrounding oxygen octahedra in NdFeAsO, which split the tenfold degenerate magnetic multiplet of Nd $^{3+}$ into five Kramers doublets.¹⁸ This has been shown by Raman, inelastic neutron scattering, and infrared measurements on many Nd-based compounds such as Nd $_2$ O $_3$, NdGaO $_3$, Nd $_2$ CuO $_4$, Nd $_2$ BaZnO $_5$, and Nd $_2$ BaCuO $_5$, for which the crystal-field splitting varies from 100 to 700 K.²¹ As a result, the paramagnetism of Nd $^{3+}$ ions at $T < 100$ K is determined by smaller effective moments μ for the Kramers doublets.

IV. MODEL OF ANTIFERROMAGNETIC SPIN FLIP TRANSITIONS

We consider breakdown of AF by strong fields, assuming that the orbital degrees of freedom of Nd $^{3+}$ are frozen by the crystalline field, and only spin degrees of freedom contribute to M . In this case the mean-field equations, $2M_1=M_0 \tanh(\mu H_1/T)$ and $2M_2=M_0 \tanh(\mu H_2/T)$ can be written to the following parametric form:

$$z = \cosh^{-1}[(2/\theta s)\sinh s - \cosh s], \quad (2)$$

$$m = \sinh z/(\cosh z + \cosh s), \quad (3)$$

$$l = \theta s/2, \quad h = z\theta/2 + \gamma m, \quad (4)$$

which define the dimensionless magnetization $m=M/M_0$ and the order parameter $l=L/M_0$ as functions of the dimensionless field $h=\mu H/T_N$ and temperature $\theta=T/T_N$. Here the parameter s runs from 0 to $2/\theta$, and $T_N=M_0(b+a)/2$. For $T < T_N$, the AF order parameter $L(H, T)$ decreases as H increases, vanishing at the second-order phase-transition field $H=H_p$:

$$H_p = [\gamma\sqrt{1-\theta} + \theta \cosh^{-1}(1/\sqrt{\theta})]T_N/\mu, \quad (5)$$

at which $M(H_p)=M_0\sqrt{1-\theta}$. For $H > H_p$, the magnetization in the paramagnetic phase is described by

$$m = \tanh[(h - \gamma m)/\theta]. \quad (6)$$

Shown in the inset of Fig. 4 are $m(h)$ and $l(h)$ curves calculated from Eqs. (2)–(6). At low temperatures, $m(h)$ and $l(h)$ become multivalued, indicating hysteretic first-order metamagnetic transitions due to spin flip in the sublattice with m antiparallel to H .

One can immediately see a very different behavior of the mean-field $M(H)$ as compared to the observed $M_p(H)$. Indeed, all $M_p(H)$ curves exhibit downward curvatures and can be described well by the Brillouin function $M=M_0 \tanh(\mu H/T)$ with $M_0=\mu n$, $\mu=(0.67-0.85)\mu_B$, and $n=(2-3) \times 10^{22}$ cm $^{-3}$ (the full set of fit parameters is given in the caption of Fig. 4). These values of n are about two times higher than the density of Nd $^{3+}$ in NdFeAs(O,F), consistent with the crystal-field splitting of the $^4I_{9/2}$ ground term of Nd $^{3+}$ into different Kramers doublets with reduced moments similar to those for many Nd-based compounds.²¹ Yet $M_p(H)$ shows no signs of long-range AF behavior below T_c , such as

the depression of $M(H)$ at $H < H_p$ depicted in the inset of Fig. 4. For example, taking $T_N = 11$ K, $\theta = 5/11$, $\mu = 0.8\mu_B$, and $\gamma = 0.5$ in Eq. (5), we obtain the AF breakdown field $H_p \approx 16$ T at $T = 4.2$ K. However, $M(H)$ in Fig. 4(a) exhibits neither the downward curvature nor metamagnetic transitions characteristic of the mean-field behavior of $M(H)$ at $H < H_p$ while the data in Fig. 4(b) exhibit no sign of this behavior on a greater magnetic-field scale either. Therefore, long-range AF ordering in the temperature range of our measurements $4.2 < T < T_c$ is inconsistent with our data, in agreement with recent neutron powder-diffraction measurements.²² At the same time, the Brillouin function for noninteracting spins gives a good description of the observed behavior of $M(T, H)$ at $T < T_c$, particularly the saturation of $M(H)$ at higher H and the decreasing low-field slope of $M(T) \sim \mu^2 n H / T$ as T increases.

In polycrystals $M(T, H)$ should be averaged with respect to randomly oriented easy magnetization directions. In this case $\chi = \chi_{\parallel}/3 + 2\chi_{\perp}/3$, where $\chi_{\parallel} = 2(1-l^2)T_N/(a+b)[T + (1-l^2)\gamma T_N]$ and $\chi_{\perp} = 1/b$. If the in-plane AF structure is present, one can expect suppression of the AF state and local metamagnetic transitions at lower T in the grains for which the in-plane field component exceeds H_p . Also, out-of-plane spin-flip transitions may occur if the perpendicular field component exceeds $H_c = [2K/(\chi_{\perp} - \chi_{\parallel})]^{1/2}$, where K is the energy of magnetic anisotropy.¹⁸ We have observed no evidences of such transitions.

V. DISCUSSION

Based on the results presented above, we conclude that the observed $M(H)$ is likely due to paramagnetism of Nd^{3+} ions controlled by exchange interactions along the NdO planes and out-of-plane Ruderman-Kittel-Kasuya-Yosida (RKKY) interactions through the AsFe planes. These interactions could provide an AF order below $T_N = T_m/\gamma \sim 10\text{--}20$ K with $\gamma < 1$. However, the superconducting transition at $T_c > T_N$ on the AsFe planes sandwiched between NdO planes cuts off the out-of-plane interactions²³ of Nd^{3+} , reducing T_N of single Nd planes below the minimum temperature of our measurements. Since the paramagnetism of our sample is only comparable with the atomic density of Nd ions, the decisive effect of magnetic second phases such as Nd_2O_3 , Fe_2As , FeAs , and FeAs_2 can be ruled out. Indeed, scanning electron microscopy and transmission electron microscopy of our samples have shown that these phases amount to less than 10%,²⁴ well below what is required to explain the data. Nevertheless, we have measured the magnetic moment $m(H)$ of Nd_2O_3 at low T and compared it to $m(H)$ for NdFeAs(O,F) , normalizing both $m(H)$ per single Nd ion. The $m(H)$ curve for Nd_2O_3 fits right between the upper and lower branches of $m(H)$ for NdFeAs(O,F) , as shown in Fig. 5, so the paramagnetic response is indeed determined by Nd^{3+} ions no matter what phase they are in. The similarity of magnetic behavior of Nd_2O_3 and NdFeAs(O,F) can be understood given that NdFeAs(O,F) contains alternat-

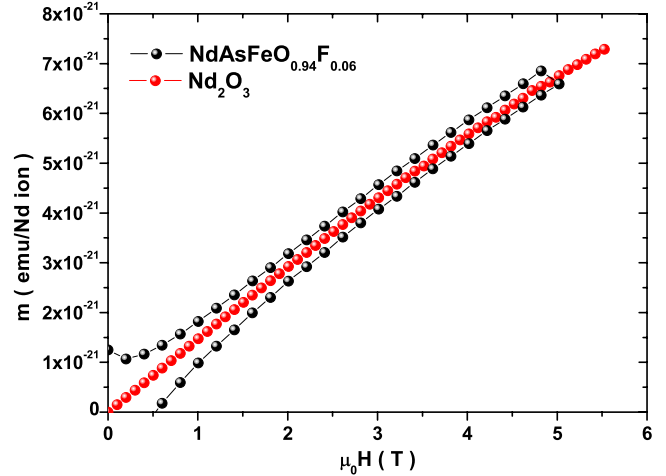


FIG. 5. (Color online) Magnetic moment per single Nd ion in $\text{NdFeAsO}_{0.94}\text{F}_{0.06}$ polycrystalline sample (black symbols) and in Nd_2O_3 [red (dark gray) symbols] as a function of applied magnetic field.

ing FeAs and NdO layers, the latter being basically a “built in” Nd oxide multilayer component with the same NdO octahedral arrangement as in Nd_2O_3 . Small admixtures of Fe_2As , FeAs , and FeAs_2 with $T_N = 353$, 77, and < 5 K, respectively,²⁵ cannot therefore change the behavior of $M(H)$ at $4 < T < 50$ K.

Our high-field data not only show that $\mu_{\text{Nd}} \gg \mu_{\text{Fe}}$ but more importantly that there is no coexistence of superconductivity and long-range AF order on the FeAs planes, at least above 4.2 K. Such long-range AF order is only possible if either $T_N < 4$ K, or $H_p > H_m = 33$ T, the latter implying T_N is much greater than T_N defined by the condition $H_p(T) = H_m$ for a given temperature T . For $\mu = 0.25\mu_B$,⁴ $T = 20$ K [the bottom curve in Fig. 4(b)], and $\gamma = 0.5$, Eq. (5) thus gives $T_N \gg 21$ K. Another possibility is a spin glass, given that $M(H)$, similar to what is shown in Fig. 4, has been observed on some metallic glasses on a much smaller field scale.²⁶ The spin glass could result from Nd^{3+} or Fe^{2+} AF clusters which may also contribute to the fractional moment $\mu < \mu_B$.

In conclusion, doped NdFeAs(O,F) can be regarded as a paramagnetic superconductor in which magnetization is dominated by the Curie-Weiss paramagnetism of Nd^{3+} . Our high-field magnetization measurements have revealed no signs of long-range antiferromagnetic order of either Nd^{3+} or Fe^{2+} below T_c despite noticeable antiferromagnetic correlations above T_c .

ACKNOWLEDGMENTS

The work at NHMFL was supported by the NSF Grant No. DMR-0084173 with additional support from the state of Florida and AFOSR (Grant No. FA9550-06-1-0474). C.T. is grateful to Eun Sang Choi for help with high-field measurements.

- ¹Y. Kamihara, T. Watanabe, M. Hirano, and H. Hosono, *J. Am. Chem. Soc.* **130**, 3296 (2008).
- ²F. Hunte, J. Jaroszynski, A. Gurevich, D. C. Larbalestier, R. Jin, A. S. Sefat, M. A. McGuire, B. C. Sales, D. K. Christen, and D. Mandrus, *Nature (London)* **453**, 903 (2008).
- ³C. de la Cruz, Q. Huang, J. W. Lynn, Jiying Li, W. Ratcliff II, J. L. Zarestky, H. A. Mook, G. F. Chen, J. L. Luo, N. L. Wang, and Pengcheng Dai, *Nature (London)* **453**, 899 (2008).
- ⁴Y. Chen, J. W. Lynn, J. Li, G. Li, G. F. Chen, J. L. Luo, N. L. Wang, Pengcheng Dai, C. dela Cruz, and H. A. Mook, *Phys. Rev. B* **78**, 064515 (2008).
- ⁵A. J. Drew, F. L. Pratt, T. Lancaster, S. J. Blundell, P. J. Baker, R. H. Liu, G. Wu, X. H. Chen, I. Watanabe, V. K. Malik, A. Dubroka, K. W. Kim, M. Rossle, and C. Bernhard, *Phys. Rev. Lett.* **101**, 097010 (2008).
- ⁶A. A. Aczel, E. Baggio-Saitovitch, S. L. Budko, P. C. Canfield, J. P. Carlo, G. F. Chen, Pengcheng Dai, T. Goko, W. Z. Hu, G. M. Luke, J. L. Luo, N. Ni, D. R. Sanchez-Candela, F. F. Tafti, N. L. Wang, T. J. Williams, W. Yu, and Y. J. Uemura, arXiv:0807.1044 (unpublished).
- ⁷K. Ahilan, F. L. Ning, T. Imai, A. S. Sefat, R. Jin, M. A. McGuire, B. C. Sales, and D. Mandrus, *Phys. Rev. B* **78**, 100501(R) (2008).
- ⁸Y. Nakai, K. Ishida, Y. Kamihara, M. Hirano, and H. Hosono, *J. Phys. Soc. Jpn.* **77**, 073701 (2008).
- ⁹G. F. Chen, Z. Li, D. Wu, G. Li, W. Z. Hu, J. Dong, P. Zheng, J. L. Luo, and N. L. Wang, *Phys. Rev. Lett.* **100**, 247002 (2008).
- ¹⁰H.-H. Wen, G. Mu, L. Fang, H. Yang, and X. Zhu, *Europhys. Lett.* **82**, 17009 (2008).
- ¹¹A. S. Sefat, M. A. McGuire, B. C. Sales, R. Jin, J. Y. Howe, and D. Mandrus, *Phys. Rev. B* **77**, 174503 (2008).
- ¹²D. J. Singh and M. H. Du, *Phys. Rev. Lett.* **100**, 237003 (2008).
- ¹³I. I. Mazin, D. J. Singh, M. D. Johannes, and M. H. Du, *Phys. Rev. Lett.* **101**, 057003 (2008).
- ¹⁴C. Cao, P. J. Hirschfeld, and H.-P. Cheng, *Phys. Rev. B* **77**, 220506(R) (2008).
- ¹⁵J. Dong, H. J. Zhang, G. Xu, Z. Li, G. Li, W. Z. Hu, D. Wu, G. F. Chen, X. Dai, J. L. Luo, Z. Fang, and N. L. Wang, *Europhys. Lett.* **83**, 27006 (2008).
- ¹⁶S. Ishibashi, K. Terakura, and H. Hosono, *J. Phys. Soc. Jpn.* **77**, 053709 (2008).
- ¹⁷J. W. Lynn, I. W. Sumarlin, S. Skanthakumar, W.-H. Li, R. N. Shelton, J. L. Peng, Z. Fisk, and S.-W. Cheong, *Phys. Rev. B* **41**, 2569(R) (1990); M. Matsuura, Pengcheng Dai, H. J. Kang, J. W. Lynn, D. N. Argyriou, K. Prokes, Y. Onose, and Y. Tokura, *ibid.* **68**, 144503 (2003); M. Matsuura, Pengcheng Dai, H. J. Kang, J. W. Lynn, D. N. Argyriou, Y. Onose, and Y. Tokura, *ibid.* **69**, 104510 (2004).
- ¹⁸K. H. J. Buschow and F. R. de Boer, *Physics of Magnetism and Magnetic Materials* (Kluwer, New York, 2004).
- ¹⁹Z. A. Ren, J. Yang, W. Lu, W. Yi, X. L. Shen, Z. C. Li, G. C. Che, X. L. Dong, L. L. Sun, F. Zhou, and Z. X. Zhao, *Europhys. Lett.* **82**, 57002 (2008).
- ²⁰C. P. Bean, *Rev. Mod. Phys.* **36**, 31 (1964).
- ²¹M. Faucher, J. Dexpert-Ghys, and P. Caro, *Phys. Rev. B* **21**, 3689 (1980); S. Jandl, J.-P. Rheault, M. Poirier, A. Ait-Ouali, A. M. Lejus, and D. Vivien, *ibid.* **56**, 11600 (1997); A. Podlesnyak, S. Rosenkranz, F. Fauth, W. Marti, A. Furrer, A. Mirmelstein, and H. J. Scheel, *J. Phys.: Condens. Matter* **5**, 8973 (1993); G. Riou, S. Jandl, M. Poirier, V. Nekvasil, M. Marysko, J. Fabry, K. Jurek, M. Divis, J. Holsa, I. M. Sutjahja, A. A. Menovsky, S. N. Barilo, S. V. Shiryayev, and L. N. Kurnevich, *Phys. Rev. B* **66**, 224508 (2002); R. S. Puche, E. Climent, J. Romero de Paz, J. L. Martinez, M. A. Monge, and C. Cascales, *ibid.* **71**, 024403 (2005).
- ²²Y. Qiu, Wei Bao, Q. Huang, T. Yildirim, J. Simmons, J. W. Lynn, Y. C. Gasparovic, J. Li, M. Green, T. Wu, G. Wu, and X. H. Chen, arXiv:0806.2195 (unpublished).
- ²³A. V. Balatsky, I. Vekhter, and J.-X. Zhu, *Rev. Mod. Phys.* **78**, 373 (2006).
- ²⁴F. Kametani, A. A. Polyanskii, A. Yamamoto, J. Jiang, E. E. Hellstrom, A. Gurevich, and D. C. Larbalestier, arXiv:0809.3393 (unpublished).
- ²⁵M. Yuzuri, R. Tahara, and Y. Nakamura, *J. Phys. Soc. Jpn.* **48**, 1937 (1980).
- ²⁶K. Binder and A. P. Young, *Rev. Mod. Phys.* **58**, 801 (1986).